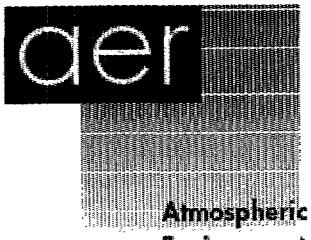

MODELING DEPOSITION OF ATMOSPHERIC MERCURY IN MICHIGAN AND THE GREAT LAKES REGION

Prepared by

Krish Vijayaraghavan

Christian Seigneur

Kristen Lohman

Shu-Yun Chen

Prakash Karamchandani

Atmospheric & Environmental Research, Inc.

2682 Bishop Drive, Suite 120

San Ramon, CA 94583

Prepared for

EPRI

3412 Hillview Avenue

Palo Alto, California 94304

Document CP184-04-02

March 2004

TABLE OF CONTENTS

LIST OF TABLES

LIST OF FIGURES

1. INTRODUCTION

This report describes the results from a modeling study conducted to investigate the fate and transport of atmospheric mercury and its deposition in Michigan and the Great Lakes region.

Mercury (Hg) is emitted into the atmosphere as gaseous or particulate species. Gaseous mercury can be either elemental, Hg(0), or divalent, Hg(II). Gaseous mercury can also adsorb to particulate matter (PM). In the atmosphere, mercury species can be converted from Hg(0) to Hg(II) and vice-versa. Most atmospheric Hg(II) occurs as inorganic compounds (with traces of organic monomethylmercury of unknown origin), while organic Hg(II) mostly occurs in water bodies.

Mercury is removed from the atmosphere via both wet deposition (precipitation) and dry deposition processes to the Earth's surface. The atmospheric lifetime of Hg(0) is believed to be on the order of several weeks. Hg(0) is not deposited rapidly to the Earth's surface and its atmospheric lifetime is, therefore, governed by oxidation to Hg(II). Gaseous Hg(II) species tend to have an atmospheric lifetime of several hours to a few days because of their high solubility in water and adsorption properties that favor their removal by wet and dry deposition. Particulate mercury is present mostly in the fine particle size section and, in the absence of precipitation, it can remain in the atmosphere for several days.

Once deposited to the Earth's surface, mercury can enter the aquatic food chain in surface water bodies where it may become methylated and bioaccumulate as methylmercury in fish. Sensitive human populations and wildlife that consume large amounts of fish may then be exposed to mercury concentrations that are potentially harmful to their health.

In this report, we first introduce the multiscale modeling system used to simulate the emissions, chemistry, transport and deposition of atmospheric mercury. The atmospheric mercury chemical kinetic mechanism employed in the model is discussed at length. We describe the model inputs including emissions, meteorology, initial and boundary conditions, and other parameters. Next, we present a performance evaluation of the modeling system by comparison with data. Then, we submit collated evidence for reduction of divalent gaseous mercury to elemental mercury in coal-fired power plant plumes. We evaluate the model again after incorporating the effect of this plume reduction. Finally, we present results from four modeling scenarios in terms of the spatial distribution of deposition fluxes of mercury and its deposition to and re-emission from the Great Lakes.

2. DESCRIPTION OF THE MODELING SYSTEM

The objective of this study is to model the atmospheric deposition of mercury (Hg) in Michigan and the Great Lakes region. Any study with such an objective must first simulate the global cycling of Hg as well as its deposition on a finer continental/regional scale. Such an approach is desirable because Hg is a global pollutant with long atmospheric residence times (Schroeder and Munthe, 1998). Therefore, the upwind boundary concentrations of mercury species are quite influential for modeling the atmospheric fate and transport of mercury at continental and regional scales. Since there is a paucity of data to specify such boundary conditions, particularly aloft, it is more reliable to obtain such boundary conditions from a global simulation, contingent upon satisfactory performance of the global model.

The multiscale modeling system used in this study consists of three nested chemical transport models (CTM): a global CTM, a continental CTM and a regional CTM. This system is "one-way": results at a given model scale drive boundary conditions at the next-smaller nested scale, but smaller scales do not determine larger-scale results. The global simulation of Hg provides the boundary conditions for modeling Hg at a continental scale. The results of the continental simulation, in turn, provide boundary conditions for modeling Hg at a regional scale. Seigneur *et al.* (2001) have described this modeling system and its initial application. The modeling system has been applied successfully in several studies of the transport and deposition of Hg over North America (Seigneur *et al.*, 2003a, 2004a, 2004b; Vijayaraghavan *et al.*, 2003, 2004). The atmospheric mercury chemistry used in the global and continental/regional CTMs in this study is described below.

2.1. Chemical Kinetic Mechanism of Atmospheric Mercury

Table 2-1 presents the atmospheric transformations among inorganic mercury species that are simulated in the multiscale modeling system. These transformations represent the current state of the science (Ryaboshapko *et al.*, 2002; Shia *et al.*, 1999; Seigneur *et al.*, 2001, 2004a, 2004b). They include the gas-phase oxidation of Hg(0) to Hg(II), the aqueous-phase oxidation of Hg(0) to Hg(II), the aqueous-phase reduction of Hg(II) to Hg(0), various aqueous-phase equilibria of Hg(II) species and the aqueous-phase adsorption of Hg(II) to PM.

Our knowledge of the atmospheric reactions of organic mercury is limited to the oxidation of dimethylmercury by OH (Niki *et al.*, 1983a), Cl (Niki *et al.*, 1983b), $O(^3P)$ (Lund-Thomsen and Egsgaard, 1986) and NO_3 (Sommar *et al.*, 1996). The first two reactions lead to the formation of monomethylmercury whereas the latter one leads to the formation of inorganic mercury. Atmospheric dimethylmercury, which originates primarily from the oceans, is rapidly converted to other species and, therefore, is not a major component of the global mercury cycle.

The atmospheric chemistry of mercury presented in Table 2-1 shows that aqueous-phase reactions (those that occur in clouds and fogs) can lead to either oxidation of Hg(0) to Hg(II) or reduction of Hg(II) to Hg(0). Such reduction-oxidation cycles affect the overall atmospheric lifetime of mercury. As mentioned above, the chemical atmospheric lifetime of Hg(0) is currently believed to be a few weeks. However, in non-precipitating clouds, Hg(II) may be reduced back to Hg(0), thereby extending the lifetime of mercury in the atmosphere. It is, therefore, important to differentiate between the chemical lifetime of a mercury species, which may range from several hours to several days for Hg(II) and Hg(p) and is several weeks for Hg(0), and the overall atmospheric lifetime of mercury (that can cycle among the various species), presently estimated to be on the order of several weeks. Further details on the mercury chemistry used in the modeling system may be found in Seigneur *et al.* (2004a).

It should be noted that there are considerable uncertainties in the current chemical kinetic mechanisms of atmospheric mercury (e.g., Ryaboshapko *et al.*, 2002) and that our knowledge of mercury chemistry continues to evolve. As new laboratory data become available, the chemical kinetic mechanism used in the modeling system is continuously updated.

2.2. Global Mercury Chemical Transport Model

The formulation of the global Hg CTM has been described in detail elsewhere (Shia *et al.*, 1999, Seigneur *et al.*, 2001, 2004a). An overview of the model is presented here.

The multiscale modeling domains used in this study are illustrated in Figure 2-1. The global Hg model is based on the three-dimensional (3-D) CTM developed at the Goddard Institute for Space Studies (GISS), Harvard University, and the University of California at Irvine. The 3-D model provides a horizontal resolution of 8° latitude and 10° longitude and a vertical resolution of nine layers ranging from the Earth's surface to the lower stratosphere. Seven layers represent the troposphere (between the surface and ~12 km altitude), and two layers the stratosphere (between ~12 km and 30 km altitude). Transport processes are driven by the wind fields and convection statistics calculated every 4 hours (for 1 year) by the GISS general circulation model (Hansen *et al.*, 1983). This 1-year data set is used repeatedly for multiyear simulations until steady state is achieved.

The Hg transformation processes include gas-phase transformations, gas/droplet equilibria, ionic equilibria, solution/particle adsorption equilibrium, and aqueous-phase transformations as described above. The chemical species reacting with Hg are input to the model as described by Seigneur *et al.* (2001). Dry and wet deposition calculations are performed as outlined by Seigneur *et al.* (2004). The global CTM provides boundary conditions for the continental/regional model that is described in the next section.

Table 2-1. Equilibria and reactions of atmospheric mercury.

Equilibrium Process or Chemical Reaction	**Equilibrium or Rate Parameter[a]**	**Reference**
$Hg(0)\,(g) \rightleftharpoons Hg(0)\,(aq)$	$0.11\ M\ atm^{-1}$	Sanemasa, 1975; Clever *et al.*, 1985
$HgCl_2\,(g) \rightleftharpoons HgCl_2\,(aq)$	$1.4 \times 10^{6}\ M\ atm^{-1}$	Lindqvist and Rodhe, 1985
$Hg(OH)_2\,(g) \rightleftharpoons Hg(OH)_2\,(aq)$	$1.2 \times 10^{4}\ M\ atm^{-1}$	Lindqvist and Rodhe, 1985
$HgCl_2\,(aq) \rightleftharpoons Hg^{2+} + 2\,Cl^-$	$10^{-14}\ M^2$	Sillen and Martell, 1964
$Hg(OH)_2\,(aq) \rightleftharpoons Hg^{2+} + 2\,OH^-$	$10^{-22}\ M^2$	Sillen and Martell, 1964
$Hg^{2+} + SO_3^{2-} \rightleftharpoons HgSO_3$	$2.1 \times 10^{13}\ M^{-1}$	van Loon *et al.*, 2001
$HgSO_3 + SO_3^{2-} \rightleftharpoons Hg(SO_3)_2^{2-}$	$1.0 \times 10^{10}\ M^{-1}$	van Loon *et al.*, 2001
$Hg(II)\,(aq) \rightleftharpoons Hg(II)\,(p)$	34 l/g	Seigneur *et al.*, 1998
$Hg(0)\,(g) + O_3\,(g) \longrightarrow Hg(II)\,(g)$	$3 \times 10^{-20}\ cm^3\ molec^{-1}s^{-1}$	Hall, 1995 [b]
$Hg(0)\,(g) + HCl(g) \longrightarrow HgCl_2(g)$	$10^{-19}\ cm^3\ molec^{-1}\ s^{-1}$	Hall and Bloom, 1993
$Hg(0)\,(g) + H_2O_2\,(g) \longrightarrow Hg(OH)_2\,(g)$	$8.5 \times 10^{-19}\ cm^3\ molec^{-1}s^{-1}$	Tokos *et al.*, 1998
$Hg(0)\,(g) + Cl_2(g) \longrightarrow HgCl_2(g)$	$2.6 \times 10^{-18}\ cm^3\ molec^{-1}s^{-1}$	Ariya *et al.*, 2002
$Hg(0)\,(g) + OH(g) \longrightarrow Hg(OH)_2(g)$	$8.0 \times 10^{-14}\ cm^3\ molec^{-1}s^{-1}$	Sommar *et al.*, 2001
$Hg(0)\,(aq) + O_3\,(aq) \longrightarrow Hg^{2+}$	$4.7 \times 10^{7}\ M^{-1}\ s^{-1}$	Munthe, 1992
$Hg(0)\,(aq) + OH\,(aq) \longrightarrow Hg^{2+}$	$2.0 \times 10^{9}\ M^{-1}\ s^{-1}$	Lin and Pehkonen, 1997
$HgSO_3\,(aq) \longrightarrow Hg(0)\,(aq)$	$0.0106\ s^{-1}$	van Loon *et al.*, 2000
$Hg(II)\,(aq) + HO_2\,(aq) \longrightarrow Hg(0)\,(aq)$	$1.7 \times 10^{4}\ M^{-1}\ s^{-1}$	Pehkonen and Lin, 1998[c]
$Hg(0)\,(aq) + HOCl\,(aq) \longrightarrow Hg^{2+}$	$2.09 \times 10^{6}\ M^{-1}\ s^{-1}$	Lin and Pehkonen, 1998
$Hg(0)\,(aq) + OCl^- \longrightarrow Hg^{2+}$	$1.99 \times 10^{6}\ M^{-1}\ s^{-1}$	Lin and Pehkonen, 1998

Hg(II) refers to divalent Hg species

[a] The parameters are for temperatures in the range of 20 to 25°C, see references for exact temperature; temperature dependence information is available for the Henry's law parameter of Hg(0) and for the kinetic rate parameter of the $HgSO_3$ reaction.

[b] The kinetics of this reaction was recently re-evaluated to be about 25 times faster by Pal and Ariya, 2004; this would lead to a greater relative contribution from Hg(0) and a lesser relative contribution of Hg(II) primary emissions to mercury deposition.

[c] This reaction was recently challenged by Gardfeldt and Johnson, 2003; however, an alternative has not been proposed

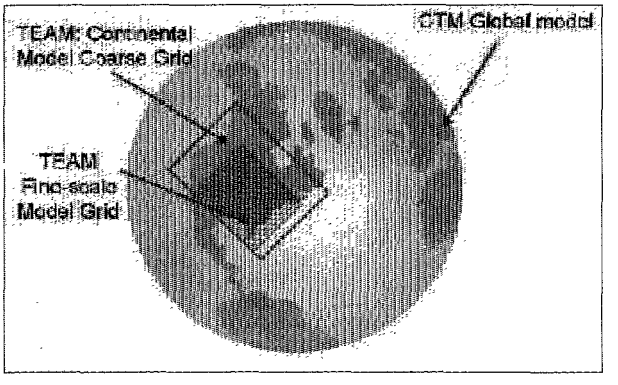

Figure 2-1: Multiscale modeling domain with global and continental/regional grids.

2.3. Continental/Regional Mercury Chemical Transport Model

The formulation of the continental/regional model, TEAM, has been described in detail elsewhere (Pai *et al.*, 1997; Seigneur *et al.*, 2001, 2004a). We present here an overview of the model.

TEAM is a 3-D Eulerian model that simulates the transport, chemical and physical transformations, wet and dry deposition of Hg species. In this application, TEAM is applied on a continental scale over North America and on a regional scale over the central and eastern United States. The regional fine grid also covers the Great Lakes region and adjoining portions of Canada. The horizontal grid resolution is 100 km for the continental grid and 20 km for the regional grid. The vertical resolution consists of six layers from the surface to 6 km altitude with finer resolution near the surface (the layer interfaces are at 60, 150, 450, 850 and 2000 m). Transport processes include transport by the 3-D mean wind flow and dispersion by atmospheric turbulence. The module that simulates the chemical and physical transformations of Hg was described above and is the same module as that used in the global model. Three Hg species, Hg(0), Hg(II) and Hg(p), are simulated. Hg(II) actually consists of several chemical species in the gas phase and in cloud droplets; Hg(II) can also adsorb to PM. The calculation of dry and wet deposition in TEAM has been described earlier (Seigneur *et al.*, 2004a; Vijayaraghavan *et al.*, 2003). The continental CTM and regional CTM are run for one datum year, in this case, 1998. Figure 2-2 shows the continental and regional nested domains with horizontal resolutions of 100 km and 20 km, respectively.

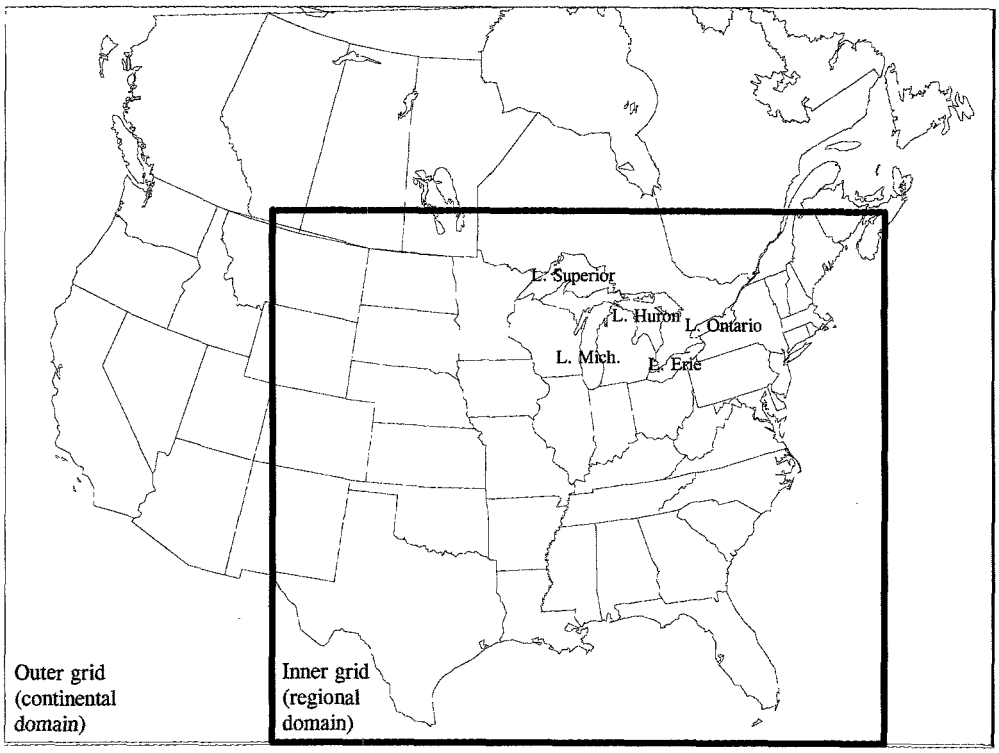

Figure 2-2. Continental and regional modeling domains (with horizontal resolution of 100 km and 20 km respectively; locations of the Great Lakes shown)

While use of a fine (20-km) grid resolution helps to better characterize the emission and fate of mercury, it should be noted that 3-D regional Eulerian models, such as this one, are not designed to simulate localized impacts of point sources at the grid-cell level as precisely as atmospheric dispersion models, which more realistically represent plume behavior due to wind and temperature. Consequently, the local impact in the model grid cell corresponding to the location of a point source is likely to be misrepresented by the regional model, as discussed in Section 5.3.

3. CONFIGURATION OF THE MODELING SYSTEM AND INPUT FILES

The global mercury CTM is run until steady state is achieved between emissions of mercury into the atmosphere and deposition to the earth, while the continental/regional models are each run for one year. The modeling year for the base case applications in this study is 1998. The atmospheric emissions and chemistry of mercury are the same in both global and continental/regional models. The configuration of the global mercury CTM and its input files have been discussed in the literature (Shia *et al.*, 1999; Seigneur *et al.*, 2001, 2004a). The preparation of input files for the continental/regional model, TEAM, has also been reviewed earlier (Seigneur *et al.*, 2001, 2004a; Vijayaraghavan *et al.*, 2003). A brief overview of the preparation of input for TEAM is presented below.

3.1 Emissions Inventory

The North American anthropogenic mercury emission inventory used in this modeling study has been summarized earlier (Pai *et al.*, 2000, Seigneur *et al.*, 2001, 2004a). In particular, new estimates of mercury emissions from coal-fired electric utilities were provided by EPRI (Levin, 2001). This inventory reflected the recent data on mercury coal content collected at all coal-fired power plants and stack measurements of speciated mercury conducted at over eighty power plants as part of the U.S. Environmental Protection Agency (EPA) Information Collection Request (ICR, 1999) program. The North American anthropogenic mercury emission inventory in the continental domain is summarized by source category in Table 3-1. Corresponding emissions in the regional modeling domain (over the central and eastern United States) are shown in Table 3-2. The regional domain also encompasses parts of Canada and Mexico with anthropogenic Hg emissions of 6.9 and 14.8 Mg/yr respectively. The category for waste incineration shown in Tables 3-1 and 3-2 includes municipal and medical waste incinerators. The values in parentheses represent updated Hg emissions after MACT implementation on these incinerators. These updates are discussed further in a later section. Hg emissions from commercial incinerators are included in the "other sources" category in Tables 3-1 and 3-2. This category also includes sources such as electric arc furnaces, electric lamp breakage, cement manufacturing, oil burning, wood burning, iron-ore roasting, landfills and others. Mercury emissions from electric arc furnaces are from the 1996 EPA National Emission Inventory (NEI) and are believed to be underestimated (CCC, 2004). Total Hg emissions from coal-fired electric utilities in Michigan are about 1.1 Mg/yr (of which about 45% is elemental and 55% oxidized mercury).

The background emissions of Hg(0) include natural emissions from active volcanoes and from the mercuriferous crustal formations of western North America, as well as re-emissions of deposited mercury. We assume that 50% of deposited mercury is re-emitted (see detailed discussion on re-emissions in Seigneur *et al.*, 2004a).

Table 3-3 shows the estimated global mercury emissions inventory (from Seigneur *et al.*, 2001; Seigneur *et al.*, 2004a) for comparison.

Table 3-1. Anthropogenic Hg emissions (Mg/yr) in the North American domain

Source Category	United States	Southern Canada	Northern Mexico	Total
Electric Utilities	41.5	1.3	9.9	52.7
Waste Incineration	28.8 (*8.2*[a])	(b)	(b)	28.8 (*8.2*[a])
Mobile Sources	24.8	(b)	(b)	24.8
Nonutility coal burning	12.8	(b)	(b)	12.8
Chlor-alkali facilities	6.7	0.05	(b)	6.8
Mining	6.4	0.3	(b)	6.7
Other Sources	30.9	13.0	23.6	67.5
Total	151.9 (131.3[a])	14.7	33.5	200.1 (*179.5*[a])

(a) Values in parentheses are Hg emissions after MACT implementation on incinerators
(b) included in "other sources"

Table 3-2. Anthropogenic emissions (Mg/yr) in the central and eastern United States

Source Category	Emissions
Electric utilities	39.3
Mobile sources	22.1
Non-utility coal burning	11.9
Waste incineration	27.2 (7.6[a])
Chloralkali facilities	6.1
Other	26.6
Total	133.2 (113.6[a])

(a) Values in parentheses are Hg emissions after MACT implementation on incinerators

Table 3-3. Global Hg Emissions (Mg/yr) (from [a]Seigneur, *et al.*, 2001; [b]Seigneur, *et al.*, 2004a)

Anthropogenic Emissions [a]	Total Hg
North America	205.0
South & Central America	176.2
Europe	508.3
Asia	1117.2
Africa	246.1
Oceania	48.3
Total direct anthropogenic [a]	2301.1
Natural emissions [b]	
Total (land+water)	1067

3.2 Meteorology

Meteorological fields are derived from the 3-D output of a prognostic meteorological model, the Nested Grid Model (NGM) of the National Oceanic and Atmospheric Administration (NOAA). Meteorology from 1998 is used. The NGM data set was obtained from the National Center for Atmospheric Research (NCAR, 2000). The cloud fields were also obtained from NCAR. Precipitation data were obtained from NCAR, the National Atmospheric Deposition Program (NADP)/Mercury Deposition Network (MDN), and the Canadian Climate Network and were combined to construct precipitation fields (see Seigneur *et al.*, 2001). The preparation of meteorological inputs to TEAM is described in detail elsewhere (Seigneur *et al.*, 2001).

3.3 Initial Conditions

We use constant initial conditions of 1.6 ng m^{-3}, 80 pg m^{-3}, and 10 pg m^{-3} for Hg(0), Hg(II) and Hg(p), respectively, for model layers (typically layers 1-3) in the atmospheric boundary layer. Above the boundary layer, Hg(II) and Hg(p) concentrations are allowed to decrease rapidly with height to a value of 0.1% of the boundary layer value at the model top. This decrease accounts for the effective scavenging of Hg(II) and Hg(p) by clouds. The vertical variation of Hg(0) is more gradual, to account for the fact that Hg(0) is a relatively long-lived species and has a longer residence time in the atmosphere. A spin-up period of ten days is used in each modeling run to minimize the influence of the initial conditions.

3.4 Boundary Conditions

The results of the global model simulation (Seigneur *et al.*, 2001, 2004a) are used to provide the boundary conditions for the TEAM application to North America. These boundary conditions consist of the concentrations of Hg(0), Hg(II) and Hg(p) as a function of location, height and season. The global grid cells used for these boundary conditions range from 20 to 68 degrees latitude north and from 45 to 145 degrees longitude west. Five of the nine layers in the global model extend from the surface to 6 km altitude. These layers are mapped into the six layers of TEAM. The boundary conditions vary according to season. The values simulated by the global model for January, April, July and October are used to represent winter, spring, summer and fall conditions, respectively.

The global CTM provides spatially-distributed and temporally-resolved fields of background mercury species concentrations and the continental CTM uses these background concentrations along with the mercury emissions within the continental domain to calculate mercury fate and transport at a spatial resolution finer than that of the global CTM. Results of the continental model simulation are, in turn, used to provide hourly concentrations of Hg(0), Hg(II) and Hg(p) for each boundary cell of the regional grid over the eastern United States.

3.5 Other Model Inputs

Land cover and terrain fields for the TEAM domain in polar stereographic projection were developed from the USGS Global Land Cover Characteristics database (GLCC) and global digital elevation database (GTOPO30) respectively. The chemical species reacting with Hg are obtained from 3-D CTM simulations for O_3, SO_2, OH, HO_2 and H_2O_2 or assumed based on available data for HCl, Cl_2 and PM as described by Seigneur *et al.* (2001). The concentrations of O_3, SO_2, OH, HO_2 and H_2O_2 are spatially and temporally varying. The concentrations of HCl and PM are spatially and temporally constant. The concentrations of Cl_2 are zero over land and temporally and spatially varying in the vertical direction over the oceans.

The mercury modeling system used in this study differs from that utilized by EPA in a few respects. The Regional Modeling System for Aerosols and Deposition (REMSAD) used in EPA modeling studies pre-assigns values to the boundary concentrations of Hg based on typical global background concentrations. Moreover, REMSAD uses meteorology driven by fields (winds, temperature, pressure, precipitation etc.) derived from an MM5 (the Penn State/NCAR Mesoscale Model) model simulation. Wet deposition fluxes are highly influenced by precipitation fields. TEAM uses daily precipitation fields from NCAR and refines them using annual precipitation data from the NADP/MDN database. REMSAD uses predicted precipitation fields from MM5 which may not be as accurate.

4. PERFORMANCE EVALUATION OF THE MODEL

4.1 Spatial Distribution of Mercury Deposition

The TEAM simulation of Vijayaraghavan *et al.* (2003, 2004) for 1998 was used as the base case simulation for this study. This fine-grid (20 km horizontal resolution) simulation covers the central and eastern United States, including Michigan and the Great Lakes region (see Figure 2-2 shown earlier). It uses 1998 meteorology, a 1998/1999 emission inventory developed by AER, and boundary conditions generated by a multiscale global/continental simulation (Seigneur *et al.*, 2004a).

Figure 4-1 illustrates the modeled dry, wet, and total (i.e., dry plus wet) mercury deposition fluxes in the 1998 base case simulation over the central and eastern United States. In this figure (and all others in this report), the fluxes shown exclude Hg(0) which is assumed to be eventually re-emitted and thus does not enter the watershed mercury cycle. Simulated annual dry deposition typically ranged between 5 and 25 $\mu g/m^2$ east of the Mississippi river. Dry deposition fluxes were less than 5 $\mu g/m^2$-yr over most of northern Michigan and mostly between 5 and 15 $\mu g/m^2$-yr in the central and southern parts of the state. Simulated annual dry deposition fluxes were above 15 $\mu g/m^2$-yr in some regions of the state near Detroit and on the eastern shore of Lake Michigan. Dry deposition fluxes were highest in the northeastern United States resulting from the impacts of a greater number of local/regional emission sources in the generally upwind direction. The highest simulated dry deposition was 204 $\mu g/m^2$ in Massachusetts. This is due to the impact of several municipal and medical waste incinerators nearby emitting more than 1 Mg/y of mercury. Less than 1% of the grid cells in the modeling domain have dry deposition greater than 25 $\mu g/m^2$.

Annual wet deposition was between 10 and 15 $\mu g/m^2$ in most of the eastern United States. Wet deposition fluxes were higher in Florida, and in urban areas such as Chicago, Detroit, along the Ohio River valley, and in the northeastern United States. The high fluxes result from the influence of local/regional sources (e.g., in the Northeast) or high precipitation (e.g., Florida). Less than one-half of one percent of the model grid cells have wet deposition fluxes greater than 25 $\mu g/m^2$. The highest wet deposition was 128 $\mu g/m^2$ near Baltimore, MD resulting from a combination of high local emissions (e.g., municipal waste combustor), regional contributions, and global background. Hg emissions have decreased significantly from the municipal waste incinerators in Baltimore and other locations since the modeled year (1998) due to implementation of MACT controls on that source category. The total deposition fluxes shown at the bottom of Figure 4-1 reflect the characteristics mentioned above for the wet and dry deposition fluxes.

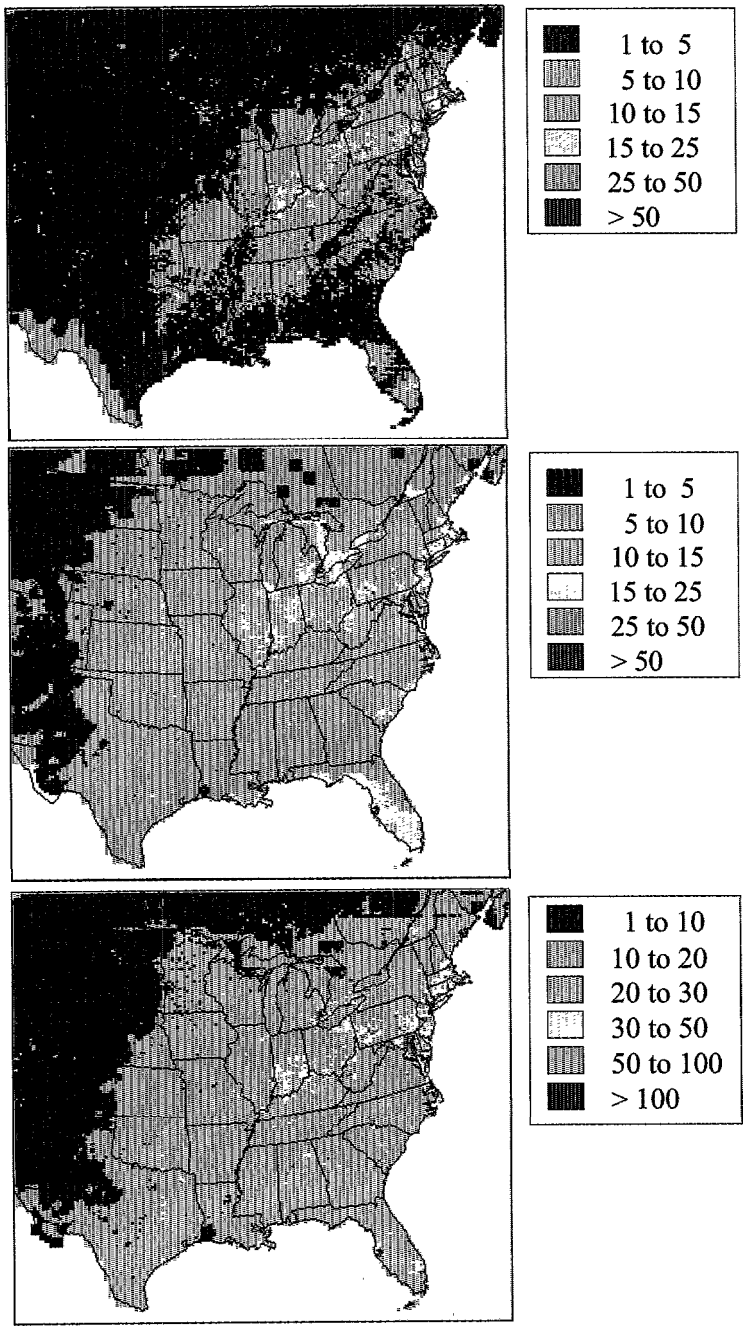

Figure 4-1. Simulated Hg dry deposition flux ($\mu g/m^2$-yr, top), wet deposition flux ($\mu g/m^2$-yr, middle), and total deposition flux ($\mu g/m^2$-yr, bottom) in the 1998 base case.

4.2 Performance Evaluation of the Base Case Simulation

A comprehensive performance evaluation of the global and continental/regional models has been conducted and presented earlier (Seigneur *et al.*, 2004a, Vijayaraghavan *et al.*, 2003). The measurements for wet deposition of mercury in 1998 in the Mercury Deposition Network (NADP/MDN, 2003) are shown in Figure 4-2. The simulated wet deposition fluxes illustrated in Figure 4-1 follow the general spatial patterns seen in the wet deposition measurements depicted in Figure 4-2. The simulated Hg wet deposition fluxes for 1998 were compared with measurements at all the MDN sites for which data were available for 1998. Note that comparisons with 2003 MDN data cannot be made unless 2003 meteorology was used in TEAM; this work was outside the scope of this study. The 1998 MDN database includes 27 sites in the United States and 3 sites in Canada. Figure 4-3 presents a comparison of simulated with measured wet deposition fluxes with a coefficient of determination (r^2) of 0.55, a normalized absolute error of 26%, and a normalized bias of 12% (normalized error = $\frac{1}{N}\sum_{i=1}^{N}\left|\frac{P_i - O_i}{O_i}\right|$; normalized bias = $\frac{1}{N}\sum_{i=1}^{N}\left(\frac{P_i - O_i}{O_i}\right)$ where P_i = prediction, O_i = observation; N: number of samples). As part of model performance evaluation, fine grid simulation results were used for MDN sites within the fine grid domain, while for stations outside this domain, the previous results of Seigneur *et al.* (2004a) were used.

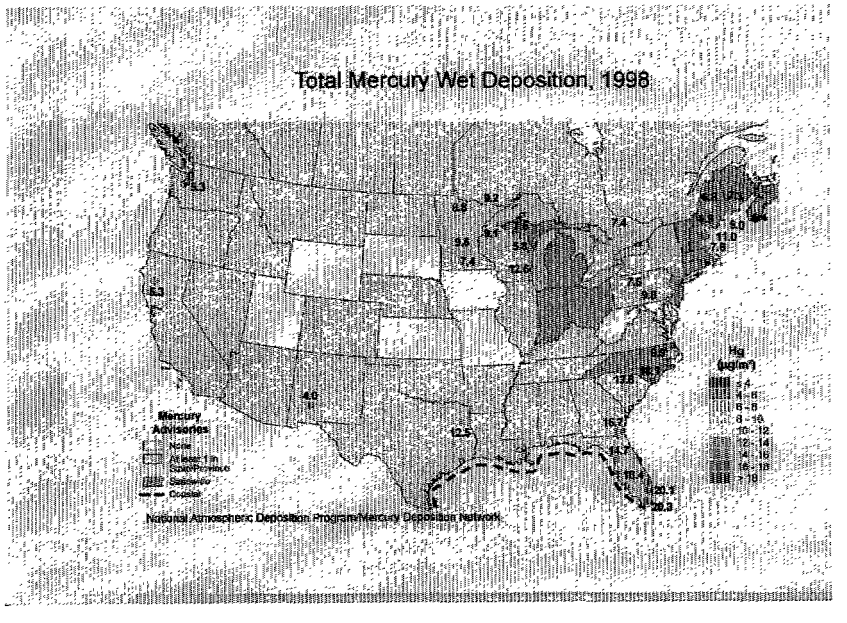

Figure 4-2. Wet deposition of Hg in 1998 at sites in the Mercury Deposition Network (NADP/MDN, 2003).

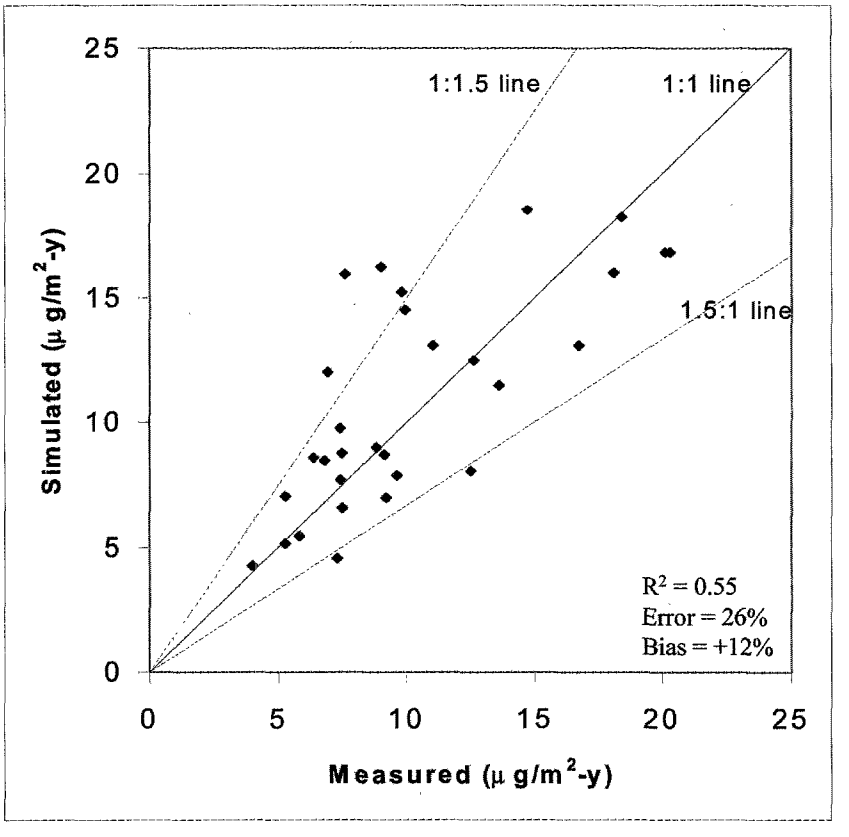

Figure 4-3. Comparison of measured and simulated Hg wet deposition fluxes ($\mu g/m^2$-yr) in 1998 at MDN sites.

A comparison of observed and simulated concentrations of atmospheric mercury is presented in Table 4-1 for several locations in the United States and Canada for which data were available for 1998. Simulated values shown in the table are either annual averages for 1998 or averages for a particular month depending on the measurement period. Reactive gaseous mercury (RGM) and total particulate mercury (TPM) are analogous to Hg(II) and Hg(p) in TEAM. In the base case simulation, the model slightly overpredicts Hg(0) and RGM while correctly estimating TPM in Chesapeake Bay. At the measurement site in Dexter, Michigan, the simulated value of total gaseous mercury (TGM, i.e., Hg(0) + Hg(II)) in 1998 is higher than the measured value in September 1998, while simulated and measured values of TPM are more comparable. In Canada, the model shows good agreement for TGM and exhibits errors between 1 and 20% at all eight sites.

Table 4-1. Comparison of observed and simulated mercury concentrations (ng/m^3).

Location	Period	Mercury species	Observation[a]	Base case simulation	Alternative speciation simulation	Reference for observation
United States						
Chesapeake Bay, MD	97-99	Hg(0)	1.89 ± 0.94	2.09	2.09	(b)
		RGM	0.04 ± 0.05	0.06	0.05	(b)
		TPM	0.02 ± 0.05	0.02	0.02	(b)
Dexter, MI	9/98	TGM	1.5 ± 0.1	2.1	2.1	(c)
		TPM	0.013 ± 0.007	0.016	0.016	(c)
Canada						
Burnt Island, ON	97-99	TGM	1.58	1.73	1.73	(d)
St. Anicet, QC	97-99	TGM	1.72	1.68	1.68	(d, e)
St. Andrews, NB	97-99	TGM	1.43	1.66	1.66	(d)
Kejimkujik, NS	97-99	TGM	1.33	1.60	1.60	(d)
Egbert, ON	97-99	TGM	1.65	1.68	1.68	(d)
Point Petre, ON	97-99	TGM	1.90	1.82	1.82	(d)
L'Assomption, QC	98	TGM	1.79	1.74	1.74	(e)
Villeroy, QC	98	TGM	1.62	1.63	1.63	(e)

(a) Mean or Mean ± Standard deviation
(b) Sheu and Mason, 2001
(c) Malcolm and Keeler, 2002
(d) Kellerhals *et al.*, 2003
(e) Poissant, 2000

4.3 Evidence for Plume Reduction of Mercury

Mercury emissions from various sources are a combination of the different speciated forms of mercury, namely, Hg(0), Hg(II) and Hg(p). The Michigan Environmental Science Board has stated in a science report on mercury in Michigan's environment (Fischer *et al.*, 1993) that there was some evidence for reduction of Hg(II) to Hg(0) in power plant plumes. Several recent experimental studies also provide direct and circumstantial evidence of reduction of Hg(II) to Hg(0) in power plant plumes. This potential reaction is very significant, because it can significantly affect deposition predictions downwind of power plants with high oxidized mercury emissions. We briefly discuss the relevant studies below.

First, the University of North Dakota Energy and Environmental Research Center and Frontier Geosciences, Inc. conducted experiments where the exhaust flue gases from a coal-fired power plant stack were sampled, diluted and analyzed in a Teflon-lined dispersion chamber. These experiments showed a lower Hg(II)/Hg(0) ratio in the chamber than in the stack (Laudal, 2001). The interpretation of those results is complicated by the fact that some Hg(II) is scavenged by the walls of the chamber. Nevertheless, the discrepancy in mercury speciation between the stack and the chamber suggests that some reactions reducing Hg(II) to Hg(0) are taking place. If such reactions also take place in the power plant plume, they would lower the mercury deposition rate and amount in the near field downwind of the source from that expected in the absence of the reactions.

Second, ambient sampling of Hg species (Hg(II), Hg(0), and Hg(p)), NO_x and SO_2 was conducted with continuous monitors downwind of coal-fired power plants in the Atlanta region (Edgerton *et al.*, 2002; Jansen, 2004). The SO_2/NO_x ratio can be used as a signature of individual power plants assuming that there is little oxidation and deposition of SO_2 and NO_x between the stacks and the sampling site. Then, the corresponding speciated mercury measurements can be compared with the mercury speciated emissions estimated from the Information Collection Request (ICR) program. The results from this study suggest that the Hg(II)/Hg(0) ratio downwind from several power plants is lower than the Hg(II)/Hg(0) ratio estimated from the ICR data for the stack emissions while total mass of Hg does not vary significantly between the two locations. An average 14% reduction per hour of Hg(II) to Hg(0) was observed across different seasons, various power plants and different plume travel times ranging up to 15 hours depending on the source and meteorological conditions.

Third, aircraft measurement campaigns performed near the Bowen plant in Georgia and the Pleasant Prairie plant in Wisconsin indicate that such conversion of Hg(II) to Hg(0) indeed takes place in power plant plumes. Preliminary results from the campaign near Bowen indicate about 40% reduction after 3 hours (Levin, 2004). There is likely more reduction for several more hours. Preliminary results from airplane measurements near Pleasant Prairie seem to indicate about 67% reduction of Hg(II) to Hg(0) in plumes at a distance of about 15 km from the stack (Laudal, 2004).

Finally, the MDN data along a west-to-east transect from Minnesota to Pennsylvania show no significant spatial gradient in mercury annual wet deposition fluxes although the Ohio Valley includes several large mercury emission sources located, under prevailing wind conditions, upwind of Pennsylvania. One potential reason is that atmospheric transformations take place that convert Hg(II) to Hg(0), thereby reducing mercury deposition since Hg(0) has an atmospheric lifetime of a few months. Note that other possible reasons include a significant contribution from dry deposition in Pennsylvania and an underestimation of mercury emissions in the upper Midwest (Seigneur *et al.*, 2003b).

4.4 Performance Evaluation of the Plume Mercury Reduction Case

An emission sensitivity simulation was conducted to incorporate the effect of reduction of Hg(II) to Hg(0) observed in power plant plumes. The speciation profile of mercury emissions from all coal-fired power plants in the central and eastern United States were modified to reflect a reduction of Hg(II) to Hg(0) in power plant plumes. We assumed that 67% of Hg(II) is reduced within a certain distance from the source (based on available experimental data described in the earlier section) and modified the emission speciation profile accordingly. The Hg(II) emissions were decreased by 67% and the Hg(0) emissions increased by the corresponding amount so that total Hg emissions remained unchanged. This change in mercury speciation corresponds to values observed far downwind in one plume from a coal-fired power plant and, therefore, is used here as an approximation for Hg(II) reduction in plumes from similar power plants. This simulation, hereafter referred to as the alternative speciation simulation, was compared to the base simulation described earlier. The percent change in dry, wet, and total deposition of Hg from the base case is illustrated in Figure 4-4. Incorporating the effect of plume mercury reduction decreases deposition by about 5% on average in central and southern Michigan. The largest impact of plume Hg(II) reduction is seen in Pennsylvania, downwind of large Hg sources in the Ohio valley, where simulated total deposition decreases by up to 59% compared to the base case.

Table 4-2 shows the effect of using the alternative emission speciation on the model performance statistics. Model performance improves on incorporating the effect of plume Hg reduction. The coefficient of determination (r^2) increases from 0.55 to 0.57, error decreased from 26% to 24%, and the bias decreased from 12% to 8%. The impact of using alternative speciation on prediction of ambient Hg concentrations is seen in Table 4-1. The fit to observed RGM improves at Chesapeake Bay while fits to Hg(0) and TPM remain unchanged. Mercury concentrations in Michigan do not change on implementing the effect of plume Hg(II) reduction. Modifying the emissions speciation of coal-fired electric utilities in the United States has no impact on simulated mercury concentrations at the measurement sites in Canada. This is likely because atmospheric mercury there is dominated by background Hg(0).

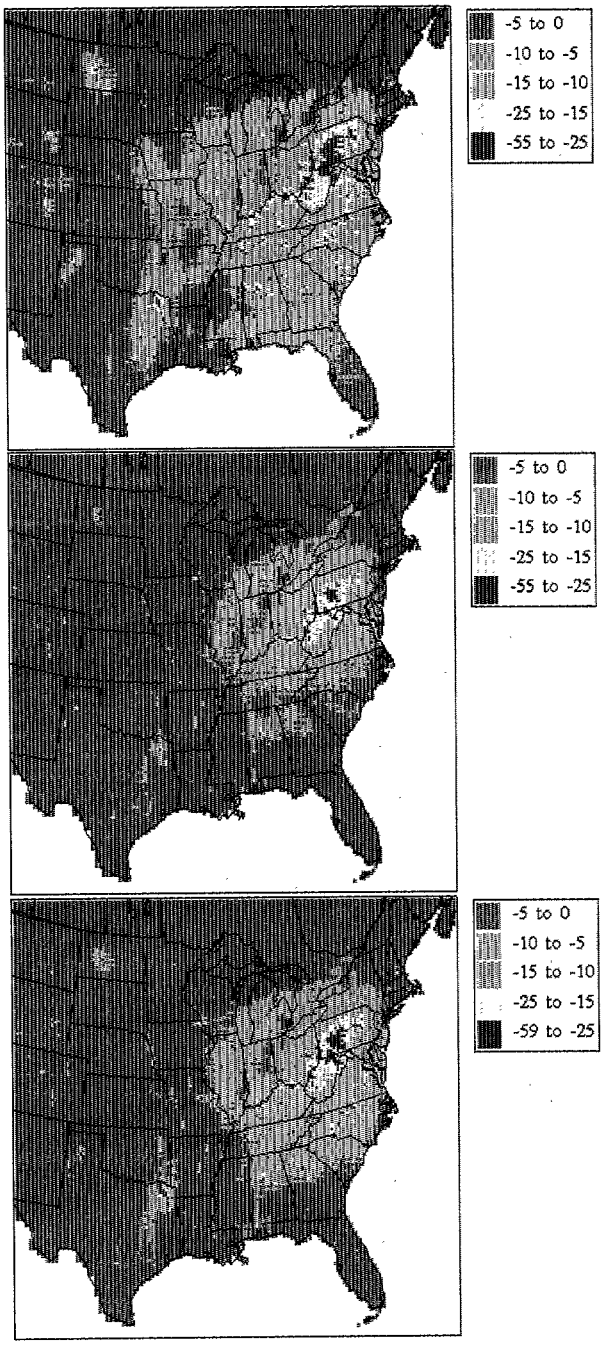

Figure 4-4. Impact of 67% reduction of Hg (II) to Hg(0) on simulated Hg dry deposition flux of Hg (top), wet deposition flux (middle), and total deposition flux (bottom).

Table 4-2. Impact of changing Hg emission speciation (i.e. incorporating the effect of plume Hg reduction) on model performance.

Performance Statistics*	Base Case	Alternative speciation
R^2	0.55	0.57
Error	26%	24%
Bias	12%	8%

* Statistics at 30 sites (for definitions, see text)

5 MODELING SCENARIOS

5.1 Simulation with Updated Incinerator Emissions

Municipal waste incinerators and medical waste incinerators have historically been major source categories for mercury emissions. The chemical speciation was studied, for example, by Dvonch *et al.* (1999) and was found to be dominated by Hg(II) (Hg(p) was not measured and was assumed to represent only 1% of the emissions). Since the chemical speciation is likely to be predominantly Hg(II), emissions from those sources should tend to deposit locally. However, the installation of emission control equipment (e.g., through the implementation of Maximum Available Control Technology, MACT) has significantly reduced incinerator emissions in the United States.

Since mercury emissions from incinerators are lower today than in our 1998 inventory, we modified the emission inventory for municipal and medical waste incinerators to reflect the implementation of MACT. We used actual stack test data for 2003 from the Michigan Department of Environmental Quality, MDEQ (Brunner, 2004) for the Detroit municipal incinerator (Greater Detroit Resource Recovery Facility). We used data from the 1999 National Emission Inventory (U.S. EPA, 2003) for information on mercury emissions from other incinerators in the country.

5.1.1 Spatial distribution of mercury deposition

A new base case simulation was conducted after updating our inventory with the new incinerator emissions data described earlier. Figure 5-1 presents the results of this new base case simulation in terms of spatial maps of annual mercury dry, wet and total deposition fluxes. Spatial patterns of mercury deposition are similar to those seen in the earlier base case shown in Figure 4-1. However, some significant decreases (~25 $\mu g/m^2$-yr) in dry deposition are simulated due to MACT implementation on incinerators in Maryland, New Jersey and Massachusetts. Wet deposition fluxes, which are also influenced by precipitation, decrease by about 5 to 10 $\mu g/m^2$-yr in these states. At the location of the Detroit municipal incinerator, the simulated dry deposition flux decreases from about 25 to 15 $\mu g/m^2$-yr. A formal statistical performance evaluation of this simulation was not conducted because of the discrepancy between the meteorological year (1998) and the more recent year(s) of the incinerator emissions.

5.1.2 Estimation of mercury deposition over the Great Lakes

The modeling domain used in this study covers all five Great Lakes. The locations of these lakes (Erie, Huron, Michigan, Ontario and Superior) in the domain are shown in Figure 2-2. The polar stereographic projection used in the model results in a distortion of the true surface area of each lake. Moreover, the contours of each lake may not be adequately captured with a grid resolution of 20 km. So, the following approach

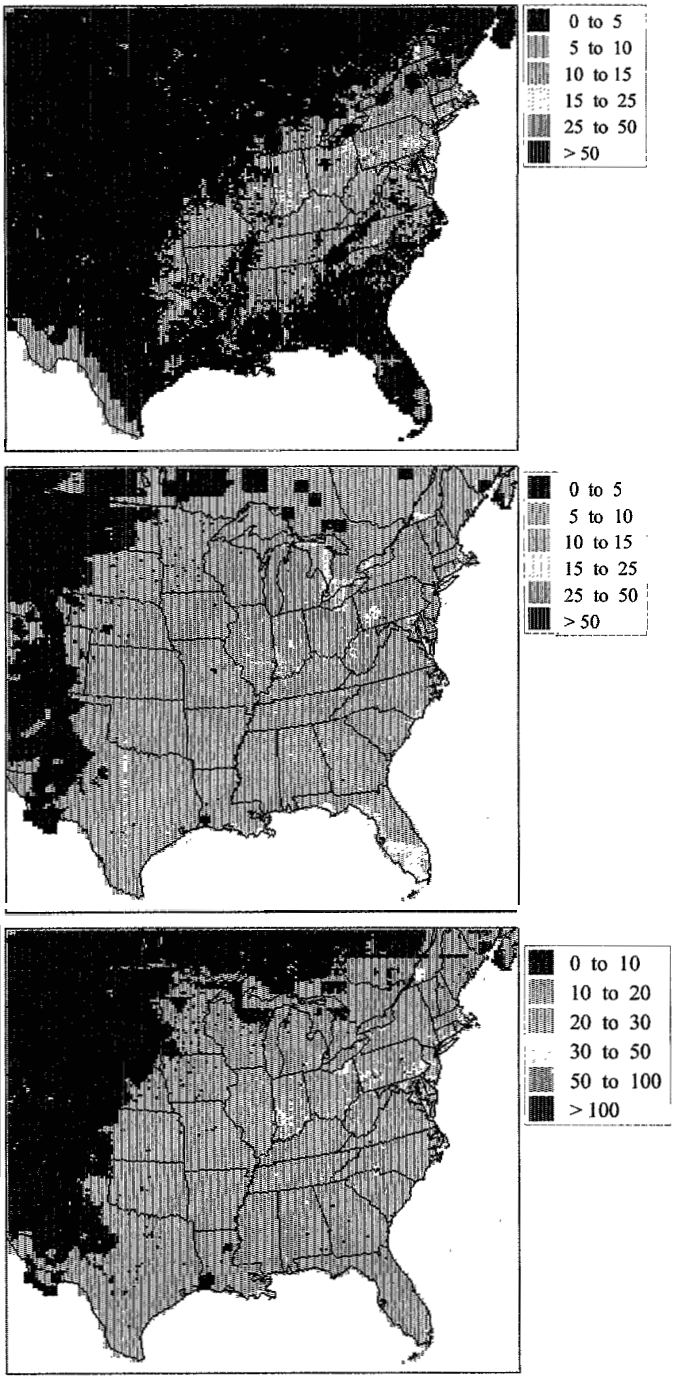

Figure 5-1. Simulated dry deposition flux of Hg ($\mu g/m^2$-yr, top), wet deposition flux ($\mu g/m^2$-yr, middle), and total deposition flux ($\mu g/m^2$-yr, bottom) in the updated base case.

was used to determine the annual wet and dry mercury deposition totals over each of the Great Lakes. The average Hg deposition flux over a lake was first calculated from the sum of the deposition fluxes over all grid cells corresponding to the lake. The average deposition flux was then multiplied by the true water surface area of the lake (U.S. Environmental Protection Agency and Government of Canada, 1995) to determine the total atmospheric deposition of mercury to the lake.

The simulated atmospheric deposition of Hg to Lake Michigan is displayed in Table 5-1. Columns 2 and 3 show the mercury deposition simulated in this study with and without MACT implementation on waste incinerators respectively. Also shown in Table 5-1 are estimates published by Landis and Keeler (2002) and Vette and co-workers (2002) for deposition to Lake Michigan during the Lake Michigan Mass Balance Study (LMMBS) from July 1994 to October 1995. Wet deposition, Hg(II) dry deposition and total deposition estimates are comparable between the current study with the 1998 inventory and that of Landis and Keeler. Re-emissions (evasion) of Hg(0) are also similar between this study and that of Landis and Keeler.

Table 5-1. Estimated atmospheric Hg deposition (kg/yr) to Lake Michigan.

Type	This study (1998 inventory + updated incinerator emissions)	This study (1998 inventory)	Landis and Keeler[a] (2002)	Vette et al.[b] (2002)
Wet deposition	582	670	614 ± 186	
Dry deposition of Hg(II)	181	236	490 ± 139	320 - 959
Dry deposition of Hg(p)	8	8	69 ± 38	
Total deposition [c]	844	988	1173 ± 235 [d]	
Re-emissions of Hg(0)	422	494	453 ± 144	286 - 797

[a] Annualized mean ± standard deviation
[b] Range of values at different ratios of RGM/TGM concentrations
[c] Total deposition also includes dry deposition of Hg(0)Range of values at different ratios of RGM/TGM concentrations
[d] Approximate standard deviation estimated from square root of sum of squares of standard deviations of components

Some differences in deposition amounts may arise because the current study simulates deposition using modeled atmospheric concentrations of Hg over the entire surface of the lake while the LMMBS calculates deposition from interpolated atmospheric measurements of Hg at 4 land-based sites around Lake Michigan and 3 over-water locations near the southern shore. Landis and Keeler have indicated that the uncertainty of their RGM dry deposition estimate is unknown and potentially large, in part because they did not measure RGM. Precipitation events could also vary between the two modeling periods (1994-95 and 1998) thus resulting in different wet deposition.

The lower value for dry deposition of Hg(p) simulated by TEAM compared to that calculated by Landis and Keeler is probably due to the following difference in dry deposition calculations. In TEAM, the dry deposition of Hg(p) is treated similarly to that of fine particles. In contrast, Landis and Keeler assign 30% of the total Hg(p) to the coarse fraction based on their size-resolved measurements; coarse particles have a higher dry deposition velocity than fine particles, thereby resulting in more particulate dry deposition. The dry deposition estimated in this study for Hg(II) is lower than the range for reactive gaseous mercury (RGM) dry deposition estimated by Vette *et al.* (2002); note, however, that Vette and co-workers did not measure RGM but estimated it from total gaseous Hg (TGM) concentration measurements. The differences between the amounts of Hg deposition simulated in this study with and without updated incinerator emissions indicate the contribution of waste incinerators to mercury deposition in Lake Michigan.

The simulated atmospheric loading of Hg to Lake Superior is shown in Table 5-2 along with estimates published by Rolfhus *et al.* (2003). The total deposition estimated in the current study is 905 kg/yr. This differs slightly from the estimate by Rolfhus and co-workers (740 kg/yr) who assumed a total (i.e. wet plus dry) flux of 9 $\mu g/m^2$-yr based on the work of Fitzgerald *et al.* (1991) at a site in northern Wisconsin. The estimated re-emissions from Lake Superior in this study are lower than the value suggested by Rolfhus and co-workers. Table 5-3 lists the estimated Hg deposition to Lake Ontario. The wet deposition of 258 kg/yr simulated by TEAM is higher than the value of 133 kg/yr estimated by the U.S. Environmental Protection Agency and Environment Canada (U.S. EPA and Environment Canada, 2002) in the 2002 Lakewide Management Plan (LaMP) report for Lake Ontario. The LaMP value is an approximate estimate based on deposition data at the two MDN stations nearest Lake Ontario. The atmospheric Hg deposition amounts to Lakes Huron and Erie simulated in the current study are shown in Tables 5-4 and 5-5. Also shown in Table 5-4 is the total deposition estimate of 500-5000 kg/yr presented at the State of the Lakes Ecosystem Conference (1994) as cited in the 2002 Lake Huron Initiative Action Plan by the Michigan Department of Environmental Quality. This is a rough approximation based on old or very limited data.

Table 5-2. Estimated atmospheric Hg deposition (kg/yr) to Lake Superior.

Type	This study (updated incinerator emissions)	Rolfhus et al. (2003)
Wet deposition	648	
Dry deposition of Hg(II)	152	
Dry deposition of Hg(p)	7	
Total deposition[(a)]	905	740
Re-emissions of Hg(0)	453	720

(a) Total deposition also includes dry deposition of Hg(0)

Table 5-3. Estimated atmospheric Hg deposition (kg/yr) to Lake Ontario.

Type	This study (updated incinerator emissions)	U.S. Environmental Protection Agency and Environment Canada (2002)
Wet deposition	258	133
Dry deposition of Hg(II)	102	
Dry deposition of Hg(p)	12	
Total deposition [a]	411	

(a) Total deposition also includes dry deposition of Hg(0)

Table 5-4. Estimated atmospheric Hg deposition (kg/yr) to Lake Huron.

Type	This study (updated incinerator emissions)	SOLEC (1994) as cited by Michigan Department of Environmental Quality (2002)
Wet deposition	717	
Dry deposition of Hg(II)	148	
Dry deposition of Hg(p)	6	
Total deposition	947 [a]	500 - 5000 [b]

(a) Total deposition also includes dry deposition of Hg(0)
(b) Rough approximation based on old or very limited data

Table 5-5. Estimated atmospheric Hg deposition (kg/yr) to Lake Erie.

Type	This study (updated incinerator emissions)
Wet deposition	373
Dry deposition of Hg(II)	132
Dry deposition of Hg(p)	9
Total deposition	556

(a) Total deposition also includes dry deposition of Hg(0)

5.2 Simulation with Updated Incinerator Emissions and Plume Mercury Reduction

An emission sensitivity simulation was conducted using updated waste incinerator emissions and alternative emissions speciation for all coal-fired power plants in the

modeling domain. The latter was implemented to reflect 67% reduction of Hg(II) to Hg(0) in power plant plumes. Figure 5-2 illustrates the simulated dry, wet, and total (i.e., dry plus wet) mercury deposition fluxes over the central and eastern United States. The percent change in total mercury deposition between this simulation and the updated base case (described in section 5.1) is depicted in Figure 5-3. Incorporating the effect of plume mercury reduction decreases total (i.e. dry plus wet) deposition of mercury by less than 10% in most of Michigan. Most of the northeastern United States exhibit more than 10% decreases with large areas in Pennsylvania, Ohio and West Virginia experiencing deposition decreases between 20 and 59%.

5.3 Simulations with No Mercury Emissions from Michigan Coal-fired Power Plants

Two emission sensitivity simulations were conducted with zero mercury emissions from all coal-fired power plants in Michigan. In the first, the original emission speciation was used for all other coal-fired power plants in the modeling domain. The second simulation employed an alternative emissions speciation for those plants to reflect 67% reduction of Hg(II) to Hg(0) in the plumes from those stacks. Note that deposition impacts from the first simulation will be an overestimate because plume mercury reduction is not considered. Comparison of the results of the second simulation with the simulation discussed in section 5.2 provides an upper-bound estimate of the effect of Michigan power plants on mercury deposition in Michigan and the Great Lakes region.

5.3.1 Impact on the spatial distribution of mercury deposition

Figure 5-4 presents the simulated percent change in total (i.e. dry+wet) mercury deposition with zero mercury emissions from all coal-fired power plants in Michigan. The top and bottom portions of the figure illustrate upper-bound estimates on mercury deposition impacts in the absence and presence of plume mercury reduction respectively. Since plume mercury reduction from power plants has been measured in several experimental studies, as described in Section 4.3, the impacts shown in the top portion of the figure are not realistic estimates; they are presented only for comparison purposes and will not be discussed further.

The northern parts of Michigan experience less than 1% decrease in total deposition of mercury when Michigan coal-fired power plant emissions are set to zero. Most parts of central and southern Michigan exhibit less than 5% decreases in total deposition of mercury. Isolated areas near Detroit, southeastern Michigan and on the eastern shore of Lake Michigan show simulated impacts on mercury deposition between 10 and 24%. Regional models of the atmospheric fate and transport of mercury, such as the one used in this study, likely over-estimate local deposition of mercury in the model grid cell corresponding to the source since they assume the plumes from point sources are instantaneously diluted in a model grid cell resulting in higher deposition closer to the source. Hence, within these 20 by 20km grid cells with large emission sources, the results provided in this study should be considered an upper-bound estimate of the effect of Michigan power plants on mercury deposition in Michigan and the Great Lakes region.

Elsewhere and over the state as a whole the model results are expected to be reasonable estimates of deposition.

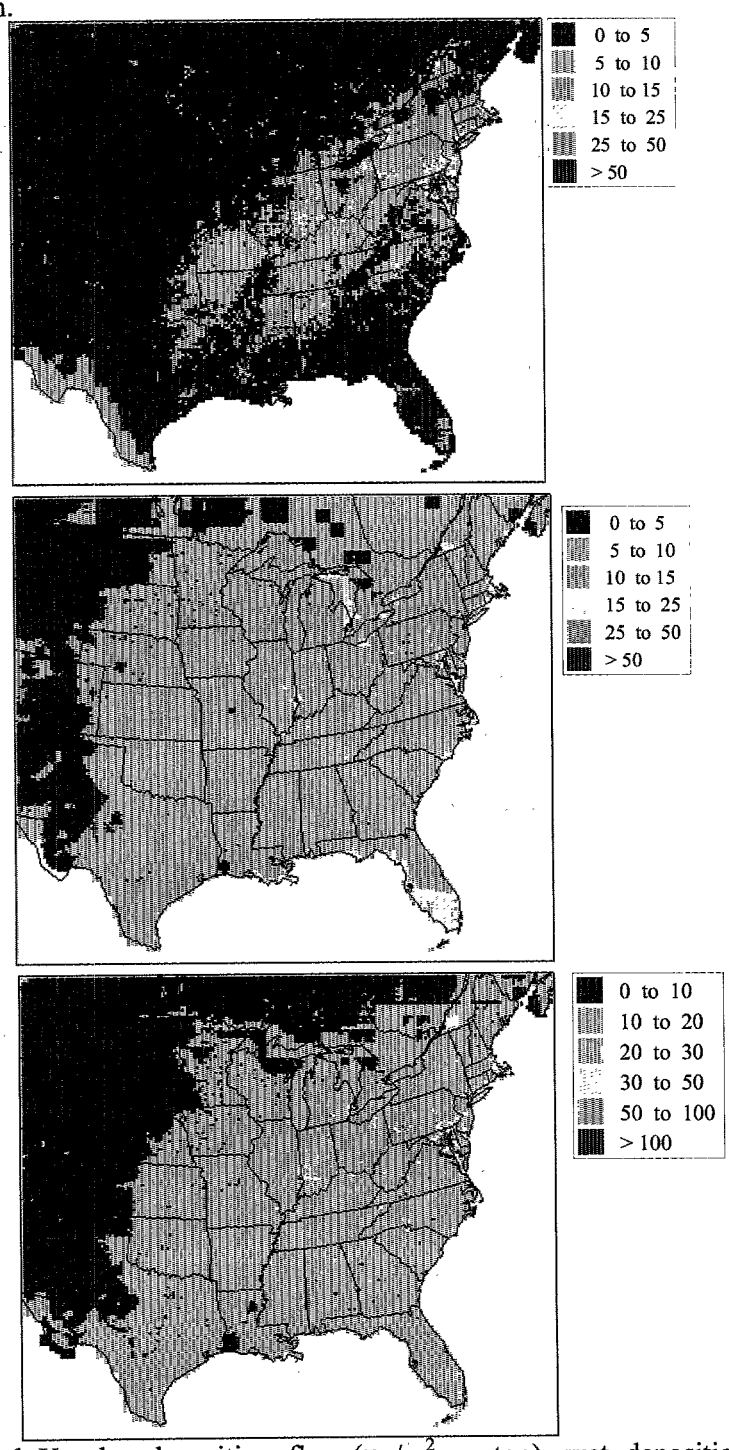

Figure 5-2. Simulated Hg dry deposition flux ($\mu g/m^2$-yr, top), wet deposition flux ($\mu g/m^2$-yr, middle), and total deposition flux ($\mu g/m^2$-yr, bottom) in the updated base case with plume Hg(II) reduction.

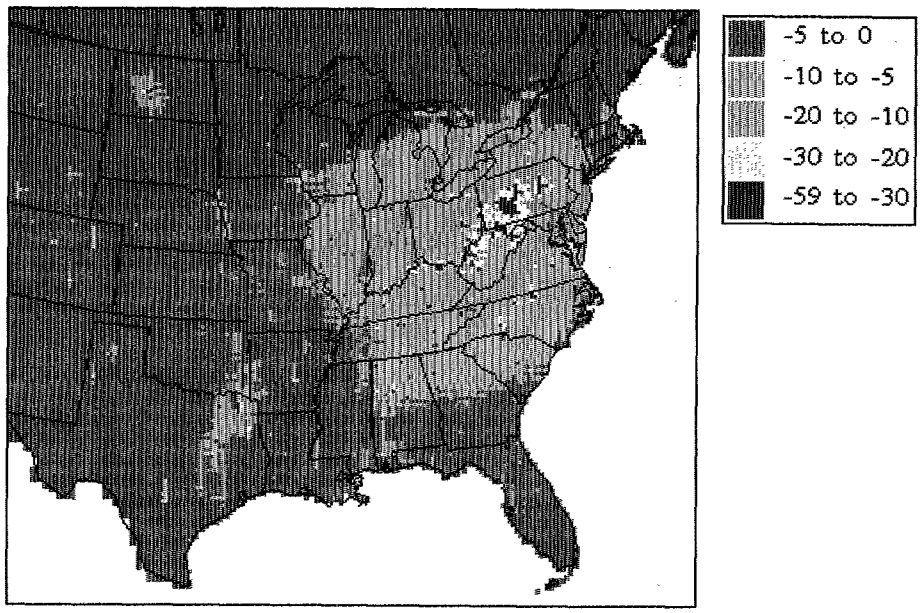

Figure 5-3. Percent change in total deposition flux of Hg between the updated base cases with and without plume Hg(II) reduction.

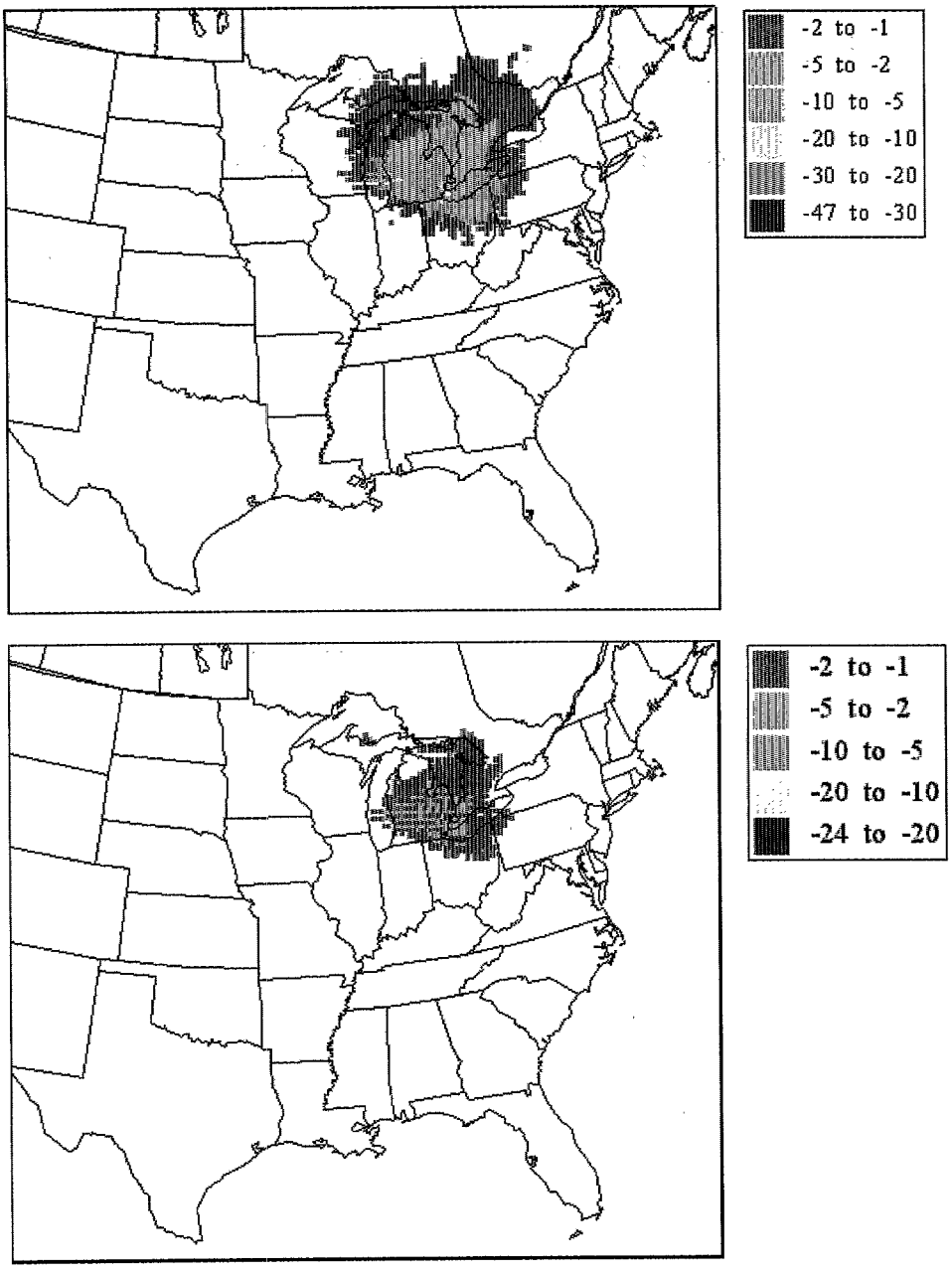

Figure 5-4. Percent change in Hg total deposition flux with zero mercury emissions from coal-fired power plants in Michigan while ignoring plume mercury reduction (top) and including plume mercury reduction (bottom) from other plants in the modeling domain. *(Note that regional Eulerian models, such as the one used in this study, overestimate mercury deposition in the immediate vicinity of large point sources due to instantaneous plume dilution)*

5.3.2 Impact on total mercury deposition over the Great Lakes

The results illustrated in the bottom half of Figure 5-4 indicate that zeroing out mercury emissions from coal-fired power plants in Michigan results in little or no impact on modeled mercury deposition fluxes in Lakes Superior and Ontario. Most parts of Lake Michigan experience negligible impact while a few areas exhibit less than 5% decrease in mercury deposition fluxes. The impact on deposition fluxes over Lake Huron is typically between 1 and 2% with a few isolated areas showing up to a 5% decrease. The majority of Lake Erie experiences decreases in deposition fluxes between 1 and 2% with some areas showing up to a 5% decrease and less than 3% of the lake experiencing between 5 and 10% impact. Table 5-6 presents a closer analysis of the estimated amounts of mercury deposited over each of the Great Lakes in the model simulations. Columns 4 and 5 show the atmospheric deposition of mercury over the lakes with and without mercury emissions from MI coal-fired electric utilities while including the effect of plume Hg reduction. Also shown for reference in columns 2 and 3 are similar values when plume Hg reduction is not considered. A comparison of columns 4 and 5 indicates that, on incorporating the effect of plume mercury reduction, mercury emissions from coal-fired power plants in Michigan contribute 0.5-1.5% to total mercury deposition over each of the Great Lakes.

Table 5-6. Estimated total atmospheric Hg deposition (kg/yr) to the Great Lakes in the modeling scenarios.

	Base Case	No Hg emissions from MI coal-fired power plants and ignoring plume Hg reduction for other power plants	Base Case including plume Hg reduction for all power plants	No Hg emissions from MI coal-fired power plants and including plume Hg reduction for other power plants
Lake Erie	556	538	490	483
Lake Huron	947	918	898	886
Lake Michigan	844	831	792	786
Lake Ontario	411	407	385	383
Lake Superior	905	897	892	886

5.3.3 Impact on total mercury deposition over Michigan

Table 5-7 presents the estimated total atmospheric mercury deposition over the state of Michigan in each of the modeling scenarios. Column 1 shows total mercury deposition over Michigan in the base case (with updated incinerator emissions) while ignoring the effect of plume mercury reduction. Column 2 lists the corresponding value

when we zero out Michigan coal-fired power plant emissions while ignoring the effect of plume mercury reduction from other power plants in the modeling domain. Column 3 presents the total deposition over Michigan in the modified base case wherein we incorporate the effect of plume mercury reduction in all coal-fired power plants in the domain. Column 4 has results from the scenario where we zero out mercury emissions from Michigan coal-fired power plants and incorporate the effect of Hg reduction in plumes from other plants in the domain. The simulations indicate that the total estimated mercury deposition over Michigan decreases from 3.95 to 3.85 Mg/yr (2.5% decrease) when we zero out Michigan coal-fired power plant emissions but ignore the effect of plume mercury reduction and from 3.82 to 3.77 Mg/yr (1.3% decrease) when we incorporate the effect of plume mercury reduction. Thus coal-fired power plants in Michigan are estimated to contribute between 1 and 3% to total mercury deposition within the state. More than 97% of mercury deposited in Michigan is a combination of deposition estimated due to emissions from: (a) non-power plant sources in Michigan, (b) mercury sources outside Michigan such as those in other states in the United States, in Canada and from the global background, and (c) natural sources in North America and elsewhere.

Table 5-7. Estimated total atmospheric Hg deposition (Mg/yr) over Michigan in the modeling scenarios

Base Case	No Hg emissions from MI coal-fired power plants and ignoring plume Hg reduction for other power plants	Base Case including plume Hg reduction for all power plants	No Hg emissions from MI coal-fired power plants and including plume Hg reduction for other power plants
3.95	3.85	3.82	3.77

6 CONCLUSION

TEAM was used to conduct several one-way nested grid simulations in which a fine grid with a horizontal resolution of 20 km was imbedded within the coarse 100 km resolution grid used in previous applications (Seigneur *et al.*, 2004). Boundary conditions for the coarse grid were obtained from the results of a global mercury chemistry transport model. The coarse model grid covered North America while the high-resolution (20 km) fine grid covered the central and eastern United States including the Great Lakes region and adjoining parts of Canada. Meteorology for 1998 was used for the simulations. Utility emissions were based on data on mercury coal content collected at all coal-fired power plants and stack measurements of speciated mercury conducted at over eighty power plants as part of the U.S. Environmental Protection Agency (EPA) Information Collection Request in 1999. The spatial distributions of simulated dry, wet, and total Hg deposition fluxes were analyzed and a comparison made of model results with observations for the base case. Overall, model performance was considered satisfactory for wet deposition fluxes at MDN sites and atmospheric mercury concentrations at various locations in the United States and Canada.

Results from several recent experimental studies suggest that there is some reduction of Hg(II) to Hg(0) in coal-fired power plant plumes that is not currently simulated in mercury models. The effect of this plume reduction was approximated in this study by modifying the mercury emissions speciation from coal-fired power plants such that Hg(II) emissions were decreased by 67% and Hg(0) emissions increased accordingly. Use of this alternative emission speciation improved model performance. The coefficient of determination (r^2) improved from 0.55 to 0.57, error decreased from 26% to 24%, and the bias decreased from 12% to 8%.

An updated base case simulation was conducted after modifying the emission inventory for municipal and medical waste incinerators to reflect the implementation of MACT. Actual stack test data for 2003 from the Michigan Department of Environmental Quality (MDEQ) was used for the Detroit municipal incinerator (Greater Detroit Resource Recovery Facility). Data from the 1999 National Emission Inventory (U.S. EPA, 2003) were used for mercury emissions from other incinerators in the country. Significant decreases in simulated dry deposition (up to 25 $\mu g/m^2$-yr) occurred in Maryland, New Jersey and Massachusetts due to MACT implementation on incinerators. At the location of the Detroit municipal incinerator, the simulated dry deposition flux decreased from about 25 to 15 $\mu g/m^2$-yr.

TEAM was also used to determine the atmospheric wet, dry, and total (i.e., wet plus dry) deposition of Hg to the five Great Lakes. Wet deposition, Hg(II) dry deposition and total deposition estimates are comparable between the current study with the 1998 inventory (before MACT implementation on waste incinerators) and that of Landis and Keeler from the Lake Michigan Mass Balance Study in 1994-95. Re-emissions of Hg(0) are also similar between this study and that of Landis and Keeler. Some differences in deposition estimates over the Great Lakes between this study and others in the literature

are believed to be due to differences in the modeling time period and the methodology used to estimate total deposition over the lake.

An emission sensitivity simulation was conducted using updated waste incinerator emissions and alternative emissions speciation for all coal-fired power plants in the modeling domain. Two additional emission sensitivity simulations were conducted with no mercury emissions from all coal-fired power plants in Michigan. In the first, the original emission speciation was used for all other coal-fired power plants in the modeling domain. The second simulation employed an alternative emissions speciation for those plants to reflect 67% reduction of Hg(II) to Hg(0) in the plumes from those utilities. Deposition impacts from the first simulation will be an overestimate because observed plume mercury reduction is not included; hence, the second simulation was used to provide an upper-bound estimate of the contribution of Michigan power plants to mercury deposition in Michigan and the Great Lakes region.

Mercury emissions from Michigan coal-fired power plants contribute less than 2% to mercury deposition fluxes in northern Michigan and less than 5% to deposition fluxes in central and southern Michigan. Isolated areas near Detroit, southeastern Michigan and on the eastern shore of Lake Michigan that comprise less than 3% of the state's land mass and are near major emission sources show simulated contributions to mercury deposition fluxes that are between 10 and 24%. However, the 3-D Eulerian model employed in this study likely overestimates mercury deposition in the immediate vicinity of large point sources due to the fact that the plumes are assumed to be diluted immediately within the model grid cell.

Mercury emissions from Michigan coal-fired power plants are calculated to contribute between 0.5 and 1.5% to total mercury deposition over each of the Great Lakes and about 2% statewide.

7 REFERENCES

Ariya, P.A., A. Khalizov and A. Gidas, 2002. Reactions of gaseous mercury with atomic and molecular halogens: kinetics, product studies, and atmospheric implications, *J. Phys. Chem.*, **106**, 7310-7320.

Brunner, J., 2004. private communication, Air Quality Division, Michigan Department of Environmental Quality, Lansing, Michigan.

CCC, 2004. Clean Car Campaign, Toxics in vehicles – Mercury - implications for recycling and disposal, www.cleancarcampaign.org/pdfs/eafdata.pdf.

Clever, H., S.A. Johnson and E.M. Derrick, 1985. The solubility of mercury and some sparingly soluble mercury salts in water and aqueous solutions, *J. Phys. Chem. Ref. Data*, **14**, 631-680.

Dvonch, J.T., J.R. Graney, G.J. Keeler and R.K. Stevens, 1999. Use of elemental tracers to source apportion mercury in South Florida precipitation, *Environ. Sci. Technol.*, **33**, 4522-4527.

Edgerton, E.S., Hartsell, B.E. and Jansen, J.J, 2002. Field observations of mercury partitioning in power plant plumes. Air Quality-III: Mercury, Trace Elements, and Particulate Matter, September, 2002, Arlington, Virginia.

Fischer, L.J., J.W. Bulkley, R.J. Cook, R.Y. Demers, D.T. Long, R.H. Olsen, B.J. Premo, E.O. van Ravenswaay, G.T. Wolff and K.G. Harrison. 1993. *Mercury in Michigan's Environment: Environmental and Human Health Concerns.* April, 1993. Michigan Environmental Science Board, Lansing, Michigan.

Gardfeldt, K. and M. Johnson, 2003. Is bimolecular reduction of Hg(II)-complexes possible in aqueous systems of environmental importance? *J. Phys. Chem.,* in press.

Hall, B., 1995. The gas-phase oxidation of elemental mercury by ozone, *Water Air Soil Pollut.*, **80**, 301-315.

Hall, B. and N. Bloom, 1993. Report to EPRI, Palo Alto, CA.

Hansen J, Russel G, Rind D, Stone P, Lacis A, Lebedeff S, Ruedy R, Travis L., 1983. Efficient three-dimensional global models for climate studies: Models I and II. *Mon. Weather Rev.* **111**, 609-662

ICR, 1999. Information Collection Request, U.S. Environmental Protection Agency, Research Triangle Park, NC.

Jansen J. J., 2004. Measurements and modeling of speciated mercury in power plant plumes. 7th Electric Utilities Environmental Conference: Air Quality, Global Climate Change & Renewable Energy, January 19-22, 2004, Tucson, Arizona.

Kellerhals M., S. Beauchamp, W. Belzer, P. Blanchard, F. Froude, B. Harvey, K. McDonald, M. Pilote, L. Poissant, K. Puckett, B. Schroeder, A. Steffen and R. Tordon, 2003: Temporal and Spatial Variability of Total Gaseous Mercury in Canada: Results from the Canadian Atmospheric Mercury Measurement Network (CAMNet), *Atmos. Environ.*, **37**, 1003-1011.

Landis, M.S. and G. Keeler, 2002. Atmospheric mercury deposition to Lake Michigan during the Lake Michigan Mass Balance Study, *Environ. Sci. Technol.*, **36**, 4518-4524.

Laudal, D., 2001. *Final Report for JV Task 24 – Investigation of the Fate of Mercury in a Coal Combustion Plume Using a Static Plume Dilution Chamber*, Cooperative Agreement No. DE-FC26-98FT40321; UND Fund 4727.

Laudal, D., 2004. private communication, EERC, University of North Dakota, 2004.

Levin, L., 2001. private communication, EPRI, Palo Alto, CA

Levin, L., 2004. private communication, EPRI, Palo Alto, CA

Lin, C.J. and S.O. Pehkonen, 1997. Aqueous-free radical chemistry of mercury in the presence of iron oxides and ambient aerosol, *Atmos. Environ.*, **31**, 4125-4137.

Lin, C.J. and S.O. Pehkonen, 1998. Oxidation of elemental mercury by aqueous chlorine ($HOCl/OCl^-$): Implications for tropospheric mercury chemistry, *J. Geophys. Res.*, **103**, 28093-28102.

Lindqvist, O. and H. Rodhe, 1985. Atmospheric mercury – a review, *Tellus*, **37B**, 136-159.

van Loon, L., E. Mader and S.L. Scott, 2000. Reduction of the aqueous mercuric ion by sulfite: UV spectrum of $HgSO_3$ and its intramolecular redox reactions, *J. Phys. Chem.*, **104**, 1621-1626.

van Loon, L.L., E.A. Mader and S.L. Scott, 2001. Sulfite stabilization and reduction of the aqueous mercuric ion: kinetic determination of sequential formation constants, *J. Phys. Chem.*, **105**, 3190-3195.

Lund-Thomsen, E. and H. Egsgaard, 1986. Rate of reaction of dimethylmercury with oxygen atoms in the gas phase, *Chem. Phys. Lett.*, **125**, 378-382.

Malcolm, E. G. and G. J. Keeler, 2002. Measurements of Mercury in Dew: Atmospheric Removal of Mercury Species to a Wetted Surface, *Environ. Sci. Technol.*, **36**, 2815-2821

Michigan DEQ, Wisconsin DNR and Minnesota Pollution Control Agency, 2003. Identification of atmospheric mercury sources in the Great Lakes states through an ambient monitoring program. Final Report. November, 2003.

Munthe, J., 1992. The aqueous oxidation of elemental mercury by ozone, *Atmos. Environ., Part A*, **26**, 1461-1468.

NADP/MDN, 2003. *National Atmospheric Deposition Program (NRSP-3)/Mercury Deposition Network*, NADP Program Office, Illinois State Water Survey, 2204 Griffith Drive, Champaign, IL.

NCAR, 2000. Archives supplied by the Techniques Development Laboratory, OSD, NWS, NOAA, available from the Data Support Section, Scientific Computing Division, National Center for Atmospheric Research, Boulder, CO.

Niki, H., P.D. Maker, C.M. Savage and L.P. Breitenbach, 1983a. A long-path Fourier transform study of the kinetics and mechanism for the HO-radical initiated oxidation of dimethyl mercury, *J. Phys. Chem.*, **87**, 4978-4981.

Niki, H., P.D. Maker, C.M. Savage and L.P. Breitenbach, 1983b. A Fourier transform study of the kinetics and mechanism for the reaction Cl + CH_3HgCH_3, *J. Phys. Chem.*, **87**, 3722-3723.

Pai, P., P. Karamchandani and C. Seigneur, 1997. Simulation of the regional atmospheric transport and fate of mercury using a comprehensive Eulerian model, *Atmos. Environ.*, **31**, 2717-2732.

Pai, P., D. Niemi and B. Powers, 2000. A North American inventory of anthropogenic mercury emissions, *Fuel Process. Technol.*, **65-66**, 101-115.

Pal B. and P. A. Ariya, 2004. Studies of Ozone Initiated Reactions of Gaseous Mercury: Kinetics Product Studies, and Atmospheric Implications, *J. Phys. Chem.*, 6, 572-579

Pehkonen, S.O. and C.J. Lin, 1998. Aqueous photochemistry of divalent mercury with organic acids, *J. Air Waste Manage. Assoc.*, **48**, 144-150.

Poissant, L., 2000. *Sci. Total Environ., 259*, 191-201.

Rolfhus, K. R., H. E. Sakamoto, L. B. Cleckner, R. W. Stoor, C. L. Babiarz, R. C. Back, H. Manolopoulos, and J. P. Hurley. 2003. Distribution and fluxes of Total and Methylmercury in Lake Superior. *Environ. Sci. Technol.* 37, 865-872.

Ryaboshapko, A., R. Bullock, R. Ebinghaus, I. Ilyin, K. Lohman, J. Munthe, G. Petersen, C. Seigneur and I. Wängberg, 2002. Comparison of mercury chemistry models, *Atmos. Environ.*, **36**, 3881-3898.

Sanemasa, I., 1975. The solubility of elemental mercury vapor in water, *Bull. Chem. Soc. Jpn.*, **48**, 1795-1798.

Schroeder, W.H. and J. Munthe, 1998. Atmospheric mercury – An overview, *Atmos. Environ.*, **32**, 809-822.

Seigneur, C., H. Abeck, G. Chia, M. Reinhard, N.S. Bloom, E. Prestbo and P. Saxena, 1998. Mercury adsorption to elemental carbon (soot) particles and atmospheric particulate matter, *Atmos. Environ.*, **32**, 2649-2657.

Seigneur, C., P. Karamchandani, K. Lohman, K. Vijayaraghavan and R.-L. Shia, 2001. Multiscale modeling of the atmospheric fate and transport of mercury, *J. Geophys. Res.*, **106**, 27795-27809.

Seigneur, C., K. Lohman, K. Vijayaraghavan and R.-L. Shia, 2003a. Contributions of global and regional sources to mercury deposition in New York State, *Environ. Pollut.*, **123**, 365-373.

Seigneur, C., P. Karamchandani,K. Vijayaraghavan, K. Lohman and G. Yelluru, 2003b. Scoping Study for Mercury Deposition in the Upper Midwest, www.ladco.org.

Seigneur, C., K. Vijayaraghavan, K. Lohman, P. Karamchandani and C. Scott, 2004a. Global source attribution for mercury deposition in the United States, *Environ. Sci. & Technol.*, **38(2)**, 555-569.

Seigneur, C., K. Vijayaraghavan, K. Lohman and P. Karamchandani, 2004b. Modeling the atmospheric fate and transport of mercury over North America, *Fuel Processing Technol.*, in press.

Sheu, G.-R., and R.P. Mason, 2001. *Environ. Sci. Technol.*, **35**, 1209-1216.

Shia, R.L., C. Seigneur, P. Pai, M. Ko, N.D. Sze, 1999. Global simulation of atmospheric mercury concentrations and deposition fluxes. *J. Geophys. Res.*, **104**, 23747-23760.

Sillen, G.L. and A.E. Martell, (Eds.), 1964. Stability constants of metal ion complexes, *Spec. Publ. Chem. Soc.*, **17**, 754.

SOLEC, 1994. State of the Lakes Ecosystem Conference, U.S. Environmental Protection Agency and Environment Canada, Dearborn, Michigan.

Sommar, J., M. Hallquist and E. Ljungstom, 1996. Rate of reaction between the nitrate radical and dimethylmercury in the gas phase, *Chem. Phys. Lett.*, **257**, 434-438.

Sommar, J., K. Gårdfeldt, D. Strömberg and X. Feng, 2001. A kinetic study of the gas-phase reaction between the hydroxyl radical and atomic mercury, *Atmos. Environ.*, **35**, 3049-3054.

Tokos, J.J.S., B. Hall, J.A. Calhoun and E.M. Prestbo, 1998. Homogeneous gas-phase reaction of Hg^0 with H_2O_2, O_3, CH_3I, and $(CH_3)_2S$: Implications for atmospheric Hg cycling, *Atmos. Environ.*, **32**, 823-827.

U.S. Environmental Protection Agency and Government of Canada, 1995. The Great Lakes: An Environmental Atlas and Resource Book

U.S. Environmental Protection Agency (EPA). National Emission Inventory (NEI), 2003. http://www.epa.gov/ttn/chief/net/1999inventory.html.

U.S. Environmental Protection Agency and Environment Canada, 2002. Lake Ontario Lakewide Management Plan (LaMP) Report.

Vette, A.F., M.S. Landis and G.J. Keeler, 2002. Deposition and emission of gaseous mercury to and from Lake Michigan during the Lake Michigan Mass Balance Study (July, 1994 – October, 1995), *Environ. Sci. Technol.*, **36**, 4525-4532.

Vijayaraghavan, K., C. Seigneur, K. Lohman and P. Karamchandani, 2003. Simulation of mercury deposition over the eastern United States with a fine spatial resolution. Air Quality-IV: Mercury, Trace Elements, and Particulate Matter, September 22-24, 2003, Arlington, Virginia.

Vijayaraghavan, K., C. Seigneur, K. Lohman, P. Karamchandani, L. Levin and J.J. Jansen, 2004. Modeling the impact of mercury speciation in power plant plumes on Hg deposition over the eastern United States. 7th Electric Utilities Environmental Conference: Air Quality, Global Climate Change & Renewable Energy, January 19-22, 2004, Tucson, Arizona.